

Title	Observed correlation between pulsating aurora and chorus waves at Syowa Station in Antarctica: A case study
Author(s)	Ozaki, Mitsunori; Yagitani, Satoshi; Ishizaka, Kazumasa; Shiokawa, Kazuo; Miyoshi, Yoshizumi; Kadokura, Akira; Yamagishi, Hisao; Kataoka, Ryuho; Ieda, Akimasa; Ebihara, Yusuke; Sato, Natsuo; Nagano, Isamu
Citation	Journal of Geophysical Research: Space Physics (2012), 117(A8)
Issue Date	2012-08
URL	http://hdl.handle.net/2433/193706
Right	©2012. American Geophysical Union.
Type	Journal Article
Textversion	publisher

Observed correlation between pulsating aurora and chorus waves at Syowa Station in Antarctica: A case study

Mitsunori Ozaki,¹ Satoshi Yagitani,¹ Kazumasa Ishizaka,¹ Kazuo Shiokawa,² Yoshizumi Miyoshi,² Akira Kadokura,³ Hisao Yamagishi,³ Ryuho Kataoka,⁴ Akimasa Ieda,² Yusuke Ebihara,⁵ Natsuo Sato,³ and Isamu Nagano¹

Received 21 December 2011; revised 4 July 2012; accepted 5 July 2012; published 9 August 2012.

[1] A high correlation between a pulsating auroral patch and grouped chorus waves was observed on 17 April 2006 at Syowa Station in Antarctica. The spatial distribution of aurora–chorus correlation coefficients is evaluated in order to determine the source region. A pulsating patch at the highest-correlation pixel shows a one-to-one correspondence with the intensity variation of the grouped chorus waves, consisting of successive rising-tone elements with a duration and spacing of 2–3 s and 20–30 s, respectively. The generation region of the chorus waves is estimated from the latitude and longitude dependence of the equatorial electron gyrofrequencies using the IGRF geomagnetic field model. The extent of the estimated latitude and longitude is consistent with the spatial distribution of the high-correlation aurora–chorus region. The time difference between the chorus waves and the scattered electrons is also evaluated to discuss the validity of the source region. It shows that electrons reached the ionosphere sooner than the associated chorus waves by ~ 1 s, consistent with the theoretical value for conjugate pulsating aurora generated at the equator. These results support the hypothesis that pulsating aurora is caused by pitch angle scattering of high-energy electrons by whistler mode chorus waves, via a cyclotron resonance at the equator. These results are the first ground-based observations of high correlations between a spatially extended aurora and chorus waves.

Citation: Ozaki, M., et al. (2012), Observed correlation between pulsating aurora and chorus waves at Syowa Station in Antarctica: A case study, *J. Geophys. Res.*, 117, A08211, doi:10.1029/2011JA017478.

1. Introduction

[2] Chorus waves in the ELF/VLF band (between several hundred Hz and 10 kHz) are the most common and intense whistler mode waves in the inner magnetosphere [Omura et al., 1991; Sazhin and Hayakawa, 1992, and references therein]. They are typically observed as a group of successive rising-tone elements across the dynamic spectrum. Chorus waves are classified into a lower and an upper band, with the boundary at half the equatorial electron gyrofrequency. The upper-band chorus can scatter low-energy electrons (below a few keV), while the lower-band chorus can

efficiently scatter high-energy electrons (above a few keV) into the loss cone [Ni et al., 2008; Meredith et al., 2009; Thorne et al., 2010].

[3] Energetic electrons produce various kinds of aurora. Pulsating aurora exhibits large and small patches having a quasiperiodic variation in luminosity with typical periods of a few seconds to a few tens of seconds [Yamamoto, 1988; Sato et al., 2004]. Modulated electron fluxes ranging from a few to tens of keV associated with such pulsating aurora have been observed in rocket and spacecraft experiments [Sandahl et al., 1980; McEwen et al., 1981; Sato et al., 2004; Nishiyama et al., 2011]. Previous studies deduced that the modulation region is located near the magnetic equator based on two types of analyses: time-of-flight analyses using the velocity dispersion of energetic electrons [Bryant et al., 1975; Smith et al., 1980; McEwen et al., 1981; Yau et al., 1981; Miyoshi et al., 2010] and observations of magnetically conjugate pulsating aurora events [Belon et al., 1969; Davis, 1978; Fujii et al., 1987]. In contrast, some studies have indicated that the modulation region is located far from the equator with nonconjugate pulsating auroral patches [Sato et al., 2004; Watanabe et al., 2007]. Certain characteristics of the source region of pulsating aurora thus remain open to discussion, but the majority of the previous studies have indicated an equatorial source. It is therefore expected that the lower-band chorus is important to the

¹Kanazawa University, Kanazawa, Japan.

²Solar-Terrestrial Environment Laboratory, Nagoya University, Nagoya, Japan.

³National Institute of Polar Research, Tokyo, Japan.

⁴Interactive Research Center of Science, Tokyo Institute of Technology, Tokyo, Japan.

⁵Research Institute for Sustainable Humanosphere, Kyoto University, Uji, Japan.

Corresponding author: M. Ozaki, Kanazawa University, Kanazawa 920-1192, Japan. (ozaki@reg.is.t.kanazawa-u.ac.jp)

©2012. American Geophysical Union. All Rights Reserved.
0148-0227/12/2011JA017478

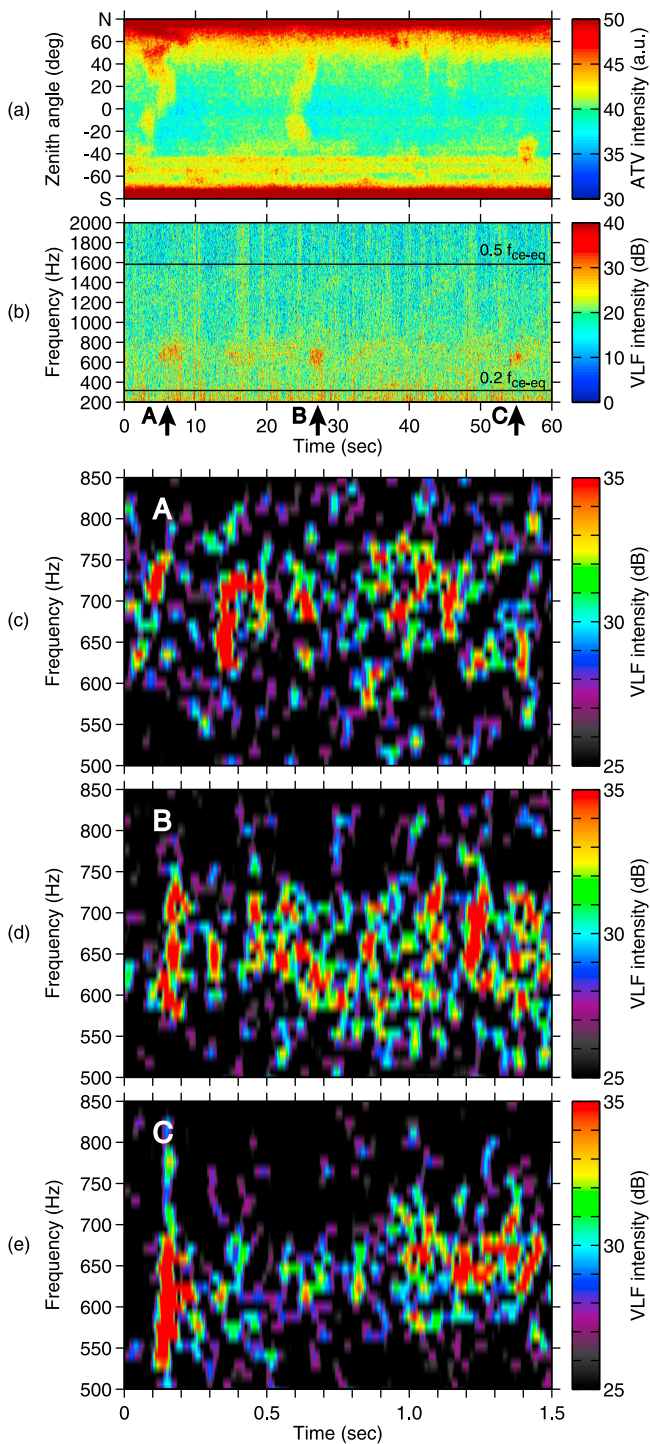


Figure 1. ATV and natural VLF wave observations on 17 April 2006. (a) ATV keogram (magnetic N–S direction) and (b) dynamic spectrum of natural VLF waves observed at 01:04:30 UT. (c–e) Dynamic spectra of rising tone chorus: group A (at 01:04:36.2 UT), B (at 01:04:55.9 UT), and C (at 01:05:23.9 UT).

precipitation of electrons causing pulsating aurora, because the energy range of this electron flux (a few to tens of keV) is more effectively scattered by the lower-band chorus than the upper-band.

[4] *Nishimura et al.* [2010, 2011] showed that the lower-band chorus observed by the THEMIS spacecraft at the magnetic equator is correlated with a pulsating auroral patch near the magnetic footprint. Ground-based observations show a one-to-one correspondence between auroral luminosity variations and chorus waves [*Tsuruda et al.*, 1981; *Hansen and Scourfield*, 1990; *Tagirov et al.*, 1999]. These studies suggest that chorus waves play an important role in understanding the generation of pulsating aurora and the related energetic electron dynamics. However, a detailed correlation analysis between auroral luminosity and chorus intensity observed on the ground has not previously been performed. The spatial distribution of auroral patches correlated with chorus waves should give information about the source region in the magnetosphere.

[5] In the present study, one particular example is presented as a case study for a correlation analysis between pulsating aurora and chorus waves observed on the ground. Ground-based observations show a strong correlation between the brightness variations of a pulsating auroral patch and the observed chorus intensity. The observed chorus waves could come from the equatorial magnetosphere or from some other source. Possible lower-band chorus frequencies were estimated from the electron gyrofrequency at the magnetospheric equatorial plane that was connected to the location of the highly correlated patches. The chorus frequency analysis demonstrates that the chorus waves fit in the range of lower-band chorus frequencies expected for an equatorial source. Therefore, it is possible that chorus waves causing pulsating aurora come from such an equatorial source.

2. Natural VLF Waves and Optical Observations

[6] Observation of natural VLF waves (generated by natural phenomena) is combined with use of a white-light all-sky TV camera (ATV) located at Syowa Station (69.0°S, 39.5°E, $L \approx 6$) in Antarctica. The ATV data were recorded on a DVD at 30 fps. The auroral images were digitized at 640×480 pixels with 8 bits of brightness. Wideband signals of the natural VLF waves were detected using a delta-type loop antenna having an area of 100 m². The VLF signals (only magnetic north-south or east-west component) and the IRIG-B time codes (for time correction) were stored in the stereo sound track of the DVD. These signals were digitized at a sampling frequency of 48 kHz with 16-bit quantization.

[7] Figures 1a and 1b show an auroral keogram along the geomagnetic north-south direction extracted from the ATV images and a dynamic spectrum of natural VLF waves observed at 01:04:30–01:05:30 UT on 17 April 2006. The 0.5 and 0.2 electron gyrofrequency lines at the magnetic equator through Syowa Station are plotted for reference on the dynamic spectrum. The universal time (local time – 3 hours) at Syowa Station is approximately the same as the magnetic local time. The event was observed during the recovery phase of a small substorm (Dst index: –27 nT, AE: 215 nT, and Kp index: 2) in the post-midnight sector. The keogram indicates repetitive intensity modulation of a few pulsating auroral patches, while the dynamic spectrum of the natural VLF waves shows intensity variations of a few grouped chorus waves in the frequency range from 600 Hz to 800 Hz. Three clear groups are seen at around 6, 27, and 55 s as indicated by the arrows. The dynamic spectra of these waves are magnified in

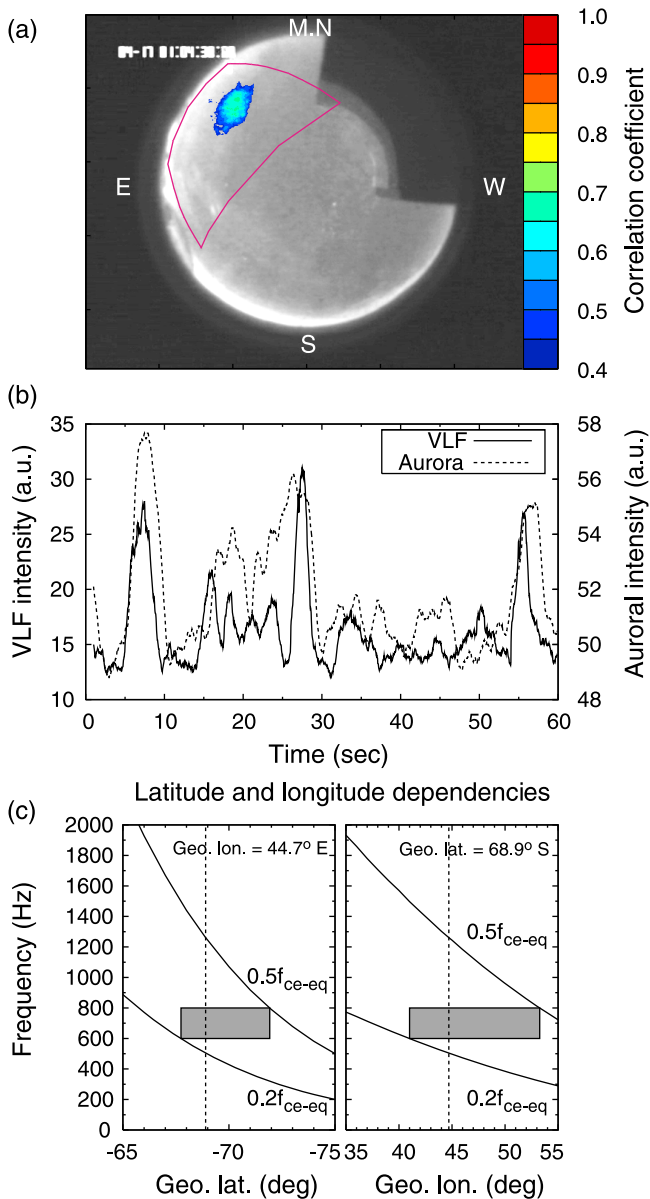


Figure 2. Correlation analysis: (a) spatial distribution of correlation coefficients between the auroral luminosity and the chorus intensity (color bars) with a chorus generation region indicated by the magenta frame estimated from the latitude and longitude dependence of the equatorial electron gyrofrequencies; (b) time variation of the observed chorus (at 600–800 Hz) and auroral intensities at the highest-correlation pixel; and (c) latitude and longitude dependence of typical chorus frequencies (between $0.2 f_{ce-eq}$ and $0.5 f_{ce-eq}$) and measured ones (600–800 Hz). The gray rectangles indicate the latitude and longitude extent of the chorus generation region. The details are explained in the text.

Figures 1c–1e. They are termed group A (at 01:04:36.2 UT), B (at 01:04:55.9 UT), and C (at 01:05:23.9 UT). Each dynamic spectrum shows successive rising-tone elements with an element duration and spacing of approximately 0.1–0.3 s, a duration of grouped elements of 2–3 s, and a spacing of each

group of 20–30 s. These features observed in the chorus wave spectra are consistent with the values for pulsating auroral patches [Yamamoto, 1988; Samara and Mitchell, 2010]. Similar results from ground-based observations suggest that a wave-particle interaction may be the generating mechanism of pulsating aurora [Tsuruda et al., 1981; Hansen and Scourfield, 1990; Tagirov et al., 1999]. The first step toward estimating the location of the source region is to determine which auroral patch is spatially related to the observed chorus waves. In section 3, a correlation analysis between the auroral luminosity and the chorus wave intensity is performed to estimate the latitude and longitude ranges for the auroral patch that is correlated with the chorus waves.

3. Spatial Aurora–Chorus Correlation and Chorus Frequency Analysis

[8] The correlation between auroral luminosity and chorus intensity was calculated for each pixel of the ATV data over the observation period 01:04:30–01:05:30 UT. Electrons interact with whistler mode waves propagating in the opposite direction via the cyclotron resonance, so that north-going (south-going) waves resonate with electrons traveling toward the southern (northern) hemisphere. The ATV data were averaged over 1.0 s (30 frames) to mitigate the effect of the time difference between the waves and electrons. A detailed analysis of the time difference is discussed in section 4. The VLF wave data was analyzed from 600 to 800 Hz to avoid impulsive atmospherics [Barr, 1970].

[9] The spatial distribution of the correlation coefficients is evident in the ATV image taken at 01:04:30 UT in Figure 2a. The high-correlation area (>0.4) is concentrated around a pulsating auroral patch. The ATV keogram (Figure 1a) does not include this highly correlated patch. Even though there were several pulsating auroral patches in the field of view of the ATV, the pixels outside this patch did not show high correlations. This correlation is consistent with previous work using the THEMIS wave data and ground-based optical images by Nishimura et al. [2010, 2011]. Figure 2b plots the auroral luminosity (dashed line) at the pixel having the highest-correlation coefficient (0.68) and the magnetic field chorus intensity (solid line). The auroral pulsations have a one-to-one correspondence with the grouped chorus generation.

[10] From previous studies [Ni et al., 2008; Thorne et al., 2010], the lower-band chorus has frequencies between $0.2 f_{ce-eq}$ and $0.5 f_{ce-eq}$, where f_{ce-eq} is the equatorial electron gyrofrequency. It is assumed that the chorus waves propagate along the geomagnetic field line passing through the highest-correlation pixel (68.9°S , 44.7°E) mapped to the equatorial plane at $L = 6.4$. A possible source region of the chorus waves was estimated from the latitude and longitude dependence of typical frequencies ($0.2 f_{ce-eq}$ and $0.5 f_{ce-eq}$) as shown in Figure 2c. The $0.2 f_{ce-eq}$ and $0.5 f_{ce-eq}$ lines are plotted by fixing either the latitude or the longitude of the highest-correlation pixel. The magnetic field line through each latitude and longitude connects to an equatorial region having a different gyrofrequency. The equatorial gyrofrequencies were calculated for the magnetic field lines connecting to the latitude or longitude of the highest-correlation pixel at an altitude of 110 km, using the 11th International Geomagnetic

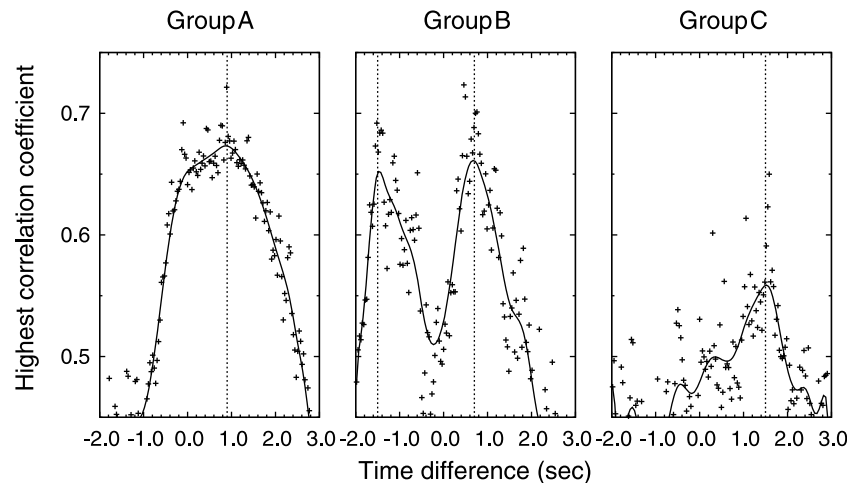


Figure 3. Highest-correlation coefficients between the auroral luminosity and the chorus intensity as a function of the time difference. Plus (minus) values indicate that electrons arrived at the ionosphere sooner (later) than the associated whistler mode waves.

Reference Field (IGRF) model [Finlay *et al.*, 2010]. The dashed lines indicate the location of the highest-correlation pixel. The observed frequency range from 600 Hz to 800 Hz lying between the two lines, for chorus frequencies calculated from the IGRF model, gives a latitude and longitude extent indicated by the gray rectangles. Setting these frequency constraints yields a generation region from 68°S to 72°S in latitude and 41°E to 53°E in longitude, projected by the magenta frame in Figure 2a. It includes the high-correlation region between the auroral and chorus intensities. The results support the conclusion that the pulsating auroral patch is driven by pitch angle scattering of energetic electrons due to chorus waves generated at the equatorial region. It is the first ground-based observation of a high-correlation region that includes a source of associated chorus waves.

4. Time Difference Between Whistler Mode Waves and Scattered Electrons

[11] Whistler mode waves interact with electrons traveling in the opposite direction. A time difference between them can be detected in ground-based VLF and optical observations from the same site. Tsuruda *et al.* [1981] and Hansen and Scourfield [1990] have suggested that the source region of pulsating aurora is localized near the equator by evaluating such time differences. To identify the time difference between VLF waves and scattered electrons, cross-correlation coefficients are calculated as a function of the time difference in the ATV data for chorus groups A (01:04:34–01:04:39 UT), B (01:04:56–01:05:00 UT), and C (01:05:23–01:05:27 UT) with a time resolution of 0.03 s. Figure 3 graphs the variations in the highest coefficient from a cross-correlation analysis among all pixels within the spatial distribution shown in Figure 2a. The time differences for these events are listed in Table 1. The symbols (“+”) and curves indicate the analytical values and Bezier curves, respectively. All three chorus events show peaks at a time difference of +1 s, indicating that the electrons reached the ionosphere sooner than the associated whistler mode waves. However, the group B event has another peak at a time difference of −1.5 s.

[12] The parallel resonance energy of electrons, E_R , for first-order cyclotron resonant scattering with whistler mode waves is [Kennel and Petschek, 1966]

$$E_R = \frac{B^2}{2\mu_0 N_e} \cdot \frac{f_{ce-eq}}{f} \cdot \left(1 - \frac{f}{f_{ce-eq}}\right)^3, \quad (1)$$

where B is the geomagnetic field intensity at the equator in units of nT, μ_0 is the vacuum permeability, N_e is the electron density in units of cm^{-3} , and f is the wave frequency. Given $B = 90$ nT, $N_e = 3 \text{ cm}^{-3}$ at the equator along the field line through the highest correlation pixel from the Global Core Plasma Model [Gallagher *et al.*, 2000], and $f = 600\text{--}800$ Hz, the parallel resonance energy is 12–7 keV, equivalent to particle velocities of 0.19–0.16 c , where c is the speed of light. These 12–7 keV electrons take 0.9–1.0 s to travel from the equator to the ionosphere (at an altitude of 110 km) along the geomagnetic field line at $L = 6.4$.

[13] The group velocity, v_{gk} , of the wave normal component of the parallel propagating whistler mode waves is [see Helliwell, 1965, chapter 3]

$$v_{gk} = 2c \cdot \frac{f^{1/2} (f_{ce-eq} \cos \theta - f)^{3/2}}{f_p f_{ce-eq} \cos \theta}, \quad (2)$$

Table 1. Observed and Theoretical Time Differences Between the Chorus Waves (at 600–800 Hz) and the Associated Electrons (at 12–7 keV)^a

Event	Time Difference (s)
Group A	+0.9 (electrons: fast)
Group B	−1.5 (waves: fast)
Group B	+0.7 (electrons: fast)
Group C	+1.5 (electrons: fast)
Case 1	−1.0 to −1.6
Case 2	+3.2 to +4.2
Case 3	+0.4 to +0.8

^aThere are two peaks for the group B event as shown in Figure 3. Plus (minus) values indicate that electrons arrived at the ionosphere sooner (later) than the associated whistler mode waves. The descriptions for the theoretical time differences in the three cases are explained in the text.

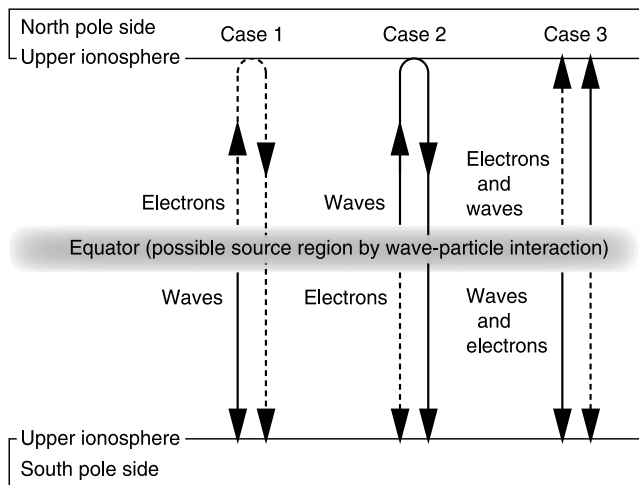


Figure 4. Three possible cases for arrival-time differences between whistler mode waves and scattered electrons.

where f_p is the plasma frequency and θ is the angle between the wave normal and the geomagnetic field. For parallel propagation ($\theta = 0$), the group velocity is $0.10\text{--}0.12c$ in the frequency range from 600 to 800 Hz. The propagation time from the equator to the ionosphere is the 1.4–1.7 s.

[14] The time difference is next calculated for three cases. Case 1 corresponds to north-going electrons reflected at the ionosphere in the opposite hemisphere. Case 2 refers to north-going whistler mode waves reflected at the ionosphere in the opposite hemisphere. Finally, case 3 denotes north- and south-going electrons and whistler mode waves that are simultaneously scattered and generated as a conjugacy event. Figure 4 illustrates the three possible scenarios for the arrival-time differences between the whistler mode waves and the scattered electrons. The time differences are -1.0 to -1.6 s for case 1, and $+3.2$ to $+4.2$ s for case 2. The observed time difference of $+1$ s does not correspond to either of these cases. Chorus waves simultaneously propagating toward the north and south from the equator have been observed by spacecraft [Santolik et al., 2003]. In case 3, the time difference is predicted to be $+0.4$ to $+0.8$ s, which is close to the observed value. The conjugacy of an aurora continues to be an unresolved issue. Watanabe et al. [2007] reported little conjugacy based on luminosity variations, but other studies reported spatial configurations of pulsating aurora at conjugate points [Belon et al., 1969; Davis, 1978; Fujii et al., 1987]. Due to simultaneous northward and southward chorus generation from the equator, the equatorial source mechanism for pulsating precipitation should scatter particles symmetrically to the northern and southern hemispheres which would imply conjugate pulsating aurora.

5. Summary

[15] A cross-correlation analysis between pulsating aurora and chorus waves has been performed based on observations on 17 April 2006 at Syowa Station in Antarctica. The analysis revealed a high-correlation region for the chorus waves. The variations in the auroral luminosity at the highest-correlation pixel show a one-to-one correspondence with the intensities of the grouped chorus waves. This result is

the first ground-based observation of a high correlation between a spatially extended aurora and chorus waves. The high-correlation region is consistent with a chorus generation region, estimated from the latitude and longitude dependence of the frequencies of the lower-band chorus ($0.2 f_{ce-eq}$ to $0.5 f_{ce-eq}$) using the IGRF model. This event therefore suggests that the modulation region of the energetic electrons causing pulsating aurora is near the equator. The time differences between the chorus waves and scattered electrons were evaluated to determine the source. It showed that the electrons reached the ionosphere approximately one second sooner than the associated whistler mode waves. This time difference is closest to the theoretical value for conjugate pulsating aurora originated from the equator. Simultaneous northward and southward chorus generation should scatter energetic particles to the northern and southern hemispheres and would contribute to viewing conjugate pulsating aurora.

[16] Previous ground-based observations have shown a one-to-one correspondence between pulsating aurora and chorus waves. Though many complex and irregular variations in the pulsating auroral patches have been simultaneously seen in the field of view, earlier studies did not quantitatively analyze which patch corresponded with which chorus waves [Tsuruda et al., 1981; Hansen and Scourfield, 1990; Tagirov et al., 1999]. This is the first ground based observational study showing a spatial relationship between a pulsating auroral patch and chorus waves using a correlation analysis. Such relationships can help determine the modulation region of the energetic electrons causing pulsating aurora. The ground-based VLF data include chorus waves incoming from various magnetospheric sources, providing better spatial coverage than satellite data. On the other hand, a high correspondence between precipitating electrons and chorus waves has seldom been detected in ground-based observations. This lack may be due to non-ducted propagation of chorus waves in the magnetosphere, wave attenuation in the Earth-ionosphere waveguide (on the order of 7 dB/100 km [Nagano et al., 1986]), collisional absorption on the order of 10–40 dB in the daytime and 1–4 dB in the nighttime ionosphere [see Helliwell, 1965, chapter 3], and reflection of chorus waves at the ionosphere.

[17] Although the present study revealed a high correlation between pulsating aurora and grouped chorus waves, as shown in Figure 2b, the correlation between each rising-tone element of the chorus waves and pulsating aurora could not be evaluated due to insufficient time and spatial resolution of the ATV images. Pulsating auroral structures have various frequencies, shapes, and spatial scales. Evaluating an imaging data set recorded using a new high-speed EMCCD camera should yield quantitative features at the relevant temporal and spatial scales [Samara and Mitchell, 2010]. Evaluating ground-based VLF data and such specific imaging methods will be the subject of a future study to investigate the relationship between auroral luminosity variations and discrete chorus elements.

[18] **Acknowledgments.** The authors thank the Japanese Antarctic Research Expedition that operated the ATV and provided natural VLF wave observations at Syowa Station. The Dst, AE, and Kp indexes were provided from WDC for Geomagnetism in Kyoto. This work was supported by a Grant-in-Aid for Scientific Research B (23403009) from the Japan Society for the Promotion of Science.

[19] Robert Lysak thanks the reviewers for their assistance in evaluating the paper.

References

- Barr, R. (1970), The attenuation of ELF and VLF radio waves propagating below inhomogeneous isotropic ionospheres, *J. Atmos. Terr. Phys.*, **32**, 1781–1791.
- Belon, A. E., J. E. Maggs, T. N. Davis, K. B. Mather, N. W. Glass, and G. F. Hughes (1969), Conjugacy of visual auroras during magnetically quiet periods, *J. Geophys. Res.*, **74**, 1–28, doi:10.1029/JA074i001p00001.
- Bryant, D. A., M. J. Smith, and G. M. Courtier (1975), Distant modulation of electron intensity during the expansion phase of an auroral substorm, *Planet. Space Sci.*, **23**, 867–878.
- Davis, T. N. (1978), Observed characteristics of auroral forms, *Space Sci. Rev.*, **22**, 77–113.
- Finlay, C. C., et al. (2010), International Geomagnetic Reference Field: The eleventh generation, *Geophys. J. Int.*, **183**, 1216–1230, doi:10.1111/j.1365-246X.2010.04804.x.
- Fujii, R., N. Sato, T. Ono, H. Fukunishi, T. Hirasawa, S. Kokubun, T. Araki, and T. Saemundsson (1987), Conjugacies of pulsating auroras by all-sky TV observations, *Geophys. Res. Lett.*, **14**, 115–118, doi:10.1029/GL014i002p00115.
- Gallagher, D. L., P. D. Craven, and R. H. Comfort (2000), Global core plasma model, *J. Geophys. Res.*, **105**, 18,819–18,833, doi:10.1029/1999JA000241.
- Hansen, H. J., and W. J. Scourfield (1990), Associated ground-based observations of optical aurorae and discrete whistler waves, *J. Geophys. Res.*, **95**, 233–239, doi:10.1029/JA095iA01p00233.
- Helliwell, R. A. (1965), *Whistlers and Related Ionospheric Phenomena*, 349 pp., Stanford Univ. Press, Stanford, Calif.
- Kennel, C. F., and H. E. Petschek (1966), Limit on stably trapped particle fluxes, *J. Geophys. Res.*, **71**, 1–28, doi:10.1029/JZ071i001p00001.
- McEwen, D. J., E. Yee, B. A. Whalen, and A. W. Yau (1981), Electron energy measurements in pulsating auroras, *Can. J. Phys.*, **59**, 1106–1115.
- Meredith, N. P., R. B. Horne, R. M. Thorne, and R. R. Anderson (2009), Survey of upper band chorus and ECH waves: Implications for the diffuse aurora, *J. Geophys. Res.*, **114**, A07218, doi:10.1029/2009JA014230.
- Miyoshi, Y., Y. Katoh, T. Nishiyama, T. Sakanoi, K. Asamura, and M. Hirahara (2010), Time of flight analysis of pulsating aurora electrons, considering wave-particle interactions with propagating whistler mode waves, *J. Geophys. Res.*, **115**, A10312, doi:10.1029/2009JA015127.
- Nagano, I., M. Mambo, T. Shimbo, and I. Kimura (1986), Intensity and polarization characteristics along the Earth's surface for the ELF–VLF waves emitted from a transmission cone in the high latitude, *Mem. Natl. Inst. Polar Res. Spec. Issue*, **42**, 34–44.
- Ni, B., R. M. Thorne, Y. Y. Shprits, and J. Bortnik (2008), Resonant scattering of plasma sheet electrons by whistler-mode chorus: Contribution to diffuse auroral precipitation, *Geophys. Res. Lett.*, **35**, L11106, doi:10.1029/2008GL034032.
- Nishimura, Y., et al. (2010), Identifying the driver of pulsating aurora, *Science*, **330**, 81–84, doi:10.1126/science.1193186.
- Nishimura, Y., et al. (2011), Multievent study of the correlation between pulsating aurora and whistler mode chorus emissions, *J. Geophys. Res.*, **116**, A11221, doi:10.1029/2011JA016876.
- Nishiyama, T., T. Sakanoi, Y. Miyoshi, Y. Katoh, K. Asamura, S. Okano, and M. Hirahara (2011), The source region and its characteristic of pulsating aurora based on the Reimei observations, *J. Geophys. Res.*, **116**, A03226, doi:10.1029/2010JA015507.
- Omura, Y., D. Nunn, H. Matsumoto, and M. J. Rycroft (1991), A review of observational, theoretical and numerical studies of VLF triggered emissions, *J. Atmos. Terr. Phys.*, **53**, 351–368.
- Samara, M., and R. G. Michell (2010), Ground-based observations of diffuse auroral frequencies in the context of whistler mode chorus, *J. Geophys. Res.*, **115**, A00F18, doi:10.1029/2009JA014852.
- Sandahl, I., L. Eliasson, and R. Lundin (1980), Rocket observations of precipitating electrons over a pulsating aurora, *Geophys. Res. Lett.*, **7**, 309–312, doi:10.1029/GL007i005p00309.
- Santolík, O., D. A. Gurnett, J. S. Pickett, M. Parrot, and N. Cornilleau-Wehrin (2003), Spatio-temporal structure of storm-time chorus, *J. Geophys. Res.*, **108**(A7), 1278, doi:10.1029/2002JA009791.
- Sato, N., D. M. Wright, C. W. Carlson, Y. Ebihara, M. Sato, T. Saemundsson, S. E. Milan, and M. Lester (2004), Generation region of pulsating aurora obtained simultaneously by the FAST satellite and a Syowa-Iceland conjugate pair of observatories, *J. Geophys. Res.*, **109**, A10201, doi:10.1029/2004JA010419.
- Sazhin, S. S., and M. Hayakawa (1992), Magnetospheric chorus emissions: A review, *Planet. Space Sci.*, **40**, 681–697.
- Smith, M. J., D. A. Bryant, and T. Edwards (1980), Pulsations in auroral electrons and positive ions, *J. Atmos. Terr. Phys.*, **42**, 167–178.
- Tagirov, V. R., V. S. Ismagilov, E. E. Titova, V. A. Arinin, A. M. Perlikov, J. Manninen, T. Turunen, and K. Kaila (1999), Auroral pulsations and accompanying VLF emissions, *Ann. Geophys.*, **17**, 66–78.
- Thorne, R. M., B. Ni, X. Tao, R. B. Horne, and N. P. Meredith (2010), Scattering by chorus waves as the dominant cause of diffuse auroral precipitation, *Nature*, **467**, 943–946, doi:10.1038/nature09467.
- Tsuruda, K., S. Machida, T. Ogoti, S. Kokubun, K. Hayashi, T. Kitamura, O. Saka, and T. Watanabe (1981), Correlations between the very low frequency chorus and pulsating aurora observed by low-light-level television at $L = 4.4$, *Can. J. Phys.*, **59**, 1042–1048.
- Watanabe, M., A. Kadokura, N. Sato, and T. Saemundsson (2007), Absence of geomagnetic conjugacy in pulsating auroras, *Geophys. Res. Lett.*, **34**, L15107, doi:10.1029/2007GL030469.
- Yamamoto, T. (1988), On the temporal fluctuations of pulsating auroral luminosity, *J. Geophys. Res.*, **93**, 897–911.
- Yau, A. W., B. A. Whalen, and D. J. McEwen (1981), Rocket-borne measurements of particle pulsation in pulsating aurora, *J. Geophys. Res.*, **86**, 5673–5681, doi:10.1029/JA086iA07p05673.